Characterization of Four-Layer Microwave Magnetic Probe Design for Integrated Circuit Emission Measurement

Hongchuan JIA [1], Fayu WAN [1], Xin CHENG [1], Vladimir MORDACHEV [2], Eugene SINKEVICH [2], Jerome ROSSIGNOL [3], Xiaohe CHEN [4], Blaise RAVELO [1]

[1] Nanjing University of Information Science & Technology (NUIST), 210044 Nanjing, Jiangsu, China
[2] Belarusian State University of Informatics and Radioelectronics, Minsk, Belarus
[3] Université de Bourgogne, Dijon, France
[4] China University of Petroleum, College of Information Science and Engineering, Beijing, China

{hongchuan.jia, fayu.wan, blaise.ravelo}@nuist.edu.cn, xinc1108@163.com, {mordachev, esinkevich}@bsuir.by, jerome.rossignol@u-bourgogne.fr, xchen@cup.edu.cn

Submitted May 6, 2025 / Accepted June 15, 2025 / Online first July 2, 2025

Abstract. *With the increase of microwave circuit and system integration design density, the test method to assess the electromagnetic compatibility (EMC) undesirable effect remains a challenging task. To tackle this issue for example with radiated emission analysis, a relevant EMC measurement notably for integrated circuits (IC) and printed circuit board (PCB) is necessary. A four-layer magnetic (H) near-field (NF) probe in miniature technology is designed, fabricated and tested. The H-NF probe works in the challenging frequency band up to 20 GHz. The proposed probe has the advantages of miniaturization, high sensitivity, high flatness, and high electric field suppression. The designed and fabricated H-NF probe characterization is validated with respect to IEC-61967 EMC standard. The device under test (DUT) IC radiation was tested and characterized. Experimental results have shown that the H-NF probe can be used for measuring IC EMC radiation emission.*

Keywords

Electromagnetic compatibility (EMC), near-field (NF) analysis, four-layer technology, magnetic NF microwave probe, design method, EMC characterization

1. Introduction

With the design technology progress, the integrated circuits (ICs) were designed with smaller size but with more complex structure by ensuring diverse RF and microwave functions. The RF and microwave electronic products integration has improved but they can also cause undesirable electromagnetic interferences (EMIs) [1–3]. Due to the widespread application of electronic products and the wireless communication network coverage, the electromagnetic (EM) environment becomes increasingly complex [4], [5]. Moreover, the problem of EMI radiated by RF and microwave communication circuits and systems is further significant [4], [5].

For this reason, nowadays, the EMI standard test of microwave devices is generally carried out in a far-field (FF) anechoic room [6]. Nevertheless, the FF testing can accurately and quantitatively measure the radiation intensity of electronic devices to determine whether they meet the requirements of the standard [6], [7]. But it cannot test the specific EM field distribution and is difficult to locate the radiation source [9], [10]. Moreover, the ICs are the main source of EMI problems in electronic devices. NF testing is a testing technique that uses NF probes to test the EM distribution in the planar surface. The NF scanning (NFS) method enables to diagnose NF radiation in ICs [10], [11], locate radiation sources [12], [13]. In addition, the NFS method is low-cost and easy to operate. It can be used in the development stage of electronic products, so it has received widespread attention. For this reason, the NFS with microwave probe design is studied in this paper.

Historically, the magnetic (H) NF probe prototype is generally a circular antenna. In 1964, the measurement effect of circular antennas on H-fields was initially proposed for the ring structure size, laying the foundation for the research of H-NF probes [14]. Early probes were mainly made of coaxial transmission lines (TLs). With the emergence of high-frequency (HF) circuits, the probe must cover the circuit working frequency. The most of printed circuit board (PCB) NFS modellings are limited to some gigahertz (GHz) [15–18]. Therefore, it is important to broaden the probe bandwidth. As coaxial lines are not suitable for HFs, broadband probes intended to operate with alternative microwave structures as such as coplanar waveguides [19], strip- [20] and coaxial- lines [21]. A team conducted a series of studies proposed an H-NF probe with a working frequency of 20 GHz in 2016 [22]. In order to improve the probe sensitivity, an active probe was proposed in 2020 [23]. In 2019,

DOI: 10.13164/re.2025.0452

a multi-component probe was designed that can simultaneously measure multiple EM field components [24]. With the rapid development of NF probes, their applications have also been popularized and developed. The NFS system can achieve automation of NF measurement. Compared with manual method, it does not only improve positioning accuracy but also saves manpower. At the same time, it can also visualize data results and obtain the distribution of EM fields on the entire plane which has great NF measurement advantages.

The components were tested at any angle using a strip line cell and found that their maximum radiation level does not always appear at the four angles specified in the IEC standard [25]. From the experimental results, it has been proven that multi-angle measurement can improve the strip line cell test accuracy for IC radiation [26], [27]. The EM radiation source of ICs was extracted by rotating the test board in a TEM cell [28]. Different measurement methods can reflect the radiation characteristics from the STM32 IC microcontroller unit (MCU) from different perspectives. Therefore, easier and efficient EMC radiation testing methods to evaluate the radiation is crucial for characterizing IC radiation issues as proposed in the present research work.

This paper is organized in four sections as follows:

- The H-NF probe intended to operate in wideband microwave frequency is studied in Sec. 2. The H-NF probe is designed in four-layer technology, fabricated and tested.
- The NFS system design as proof-of-concept (PoC), construction technique and test are explained in Sec. 3. The measurement results of H-NF radiated by a microcontroller (MCU) digital IC implemented in a prototype of printed circuit board (PCB) representing the device under test (DUT) are discussed.
- Finally, Section 4 summarizes the conclusion.

2. Design and Characterization of the Four-Layer H-NF Probe under Study

This section introduces the work principle and design of innovative H-NF miniaturized probe implemented in four-layer technology. The characterization test of H-NF probe to operate in wideband microwave frequencies is discussed.

2.1 Structure of the Four-Layer H-NF Probe

To scan a rectangular test surface in the (xy)-plan of (Oxyz) Cartesian system, the H-NF probe with operating frequency f, sensitivity and other indicators can be changed from the inner and outer conductor diameters and the tip length. Figure 1 displays the photo of the designed and fabricated microwave H-NF probe.

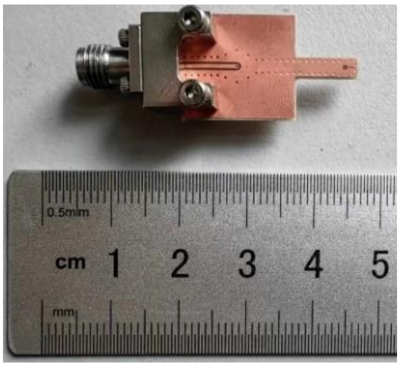

Fig. 1. Photo of the designed four-layer H-NF probe.

As laminated face view, Figure 2(a) shows the innovative H-NF probe implemented in 4-layer technology. Figure 2(b) shows the probe size parameters. $D_1 = 0.7$ mm is the distance between the center of the vias and the slot line edge and the distance between adjacent vias is $D_2 = 0.9$ mm. The H-NF probe through-hole fence at the connection end consists of a series of through-holes connected to the upper and lower grounding layers, placed on both sides of the CPWG groove line to ensure the scattering coefficient curve smoothness. Figure 2(c) represents the corresponding layered structures.

The increase in the number of through-holes improves the S_{21} smoothness. W and D_1 need to be small enough (far less than quarter-wavelength associated to the maximum operating frequency) to enhance the grounded coplanar waveguide (CPWG) structural performance. The signal propagating through the hole connects the strip and CPWG signal lines and its characteristic impedance is discontinuous.

The equivalent circuit of the signal propagating through the hole consists of parallel and series parasitic capacitors. At high frequencies, the parasitic effects are obvious and lead to serious characteristic impedance mismatch. The coaxial via array technology can enhance impedance matching, with distance $D = 2.25$ mm between the coaxial and center vias.

Description	Parameter	Value (mm)
Width	W_1	1.16
	W_2	0.56
	W_3	0.39
	WL_1	15
	WL_2	3
Hole radius	R_1	0.3
Sensor unit	W_k	0.6
Hole arrangement	R_2	2.25
	D_1	0.7
	D_2	0.9
	D_3	0.7
	α	45°
TL length	L_1	7.65
	L_2	15.9
	L_3	5
	L_h	3.98

Tab. 1. Physical design parameters of the NF probe prototype shown in Fig. 2.

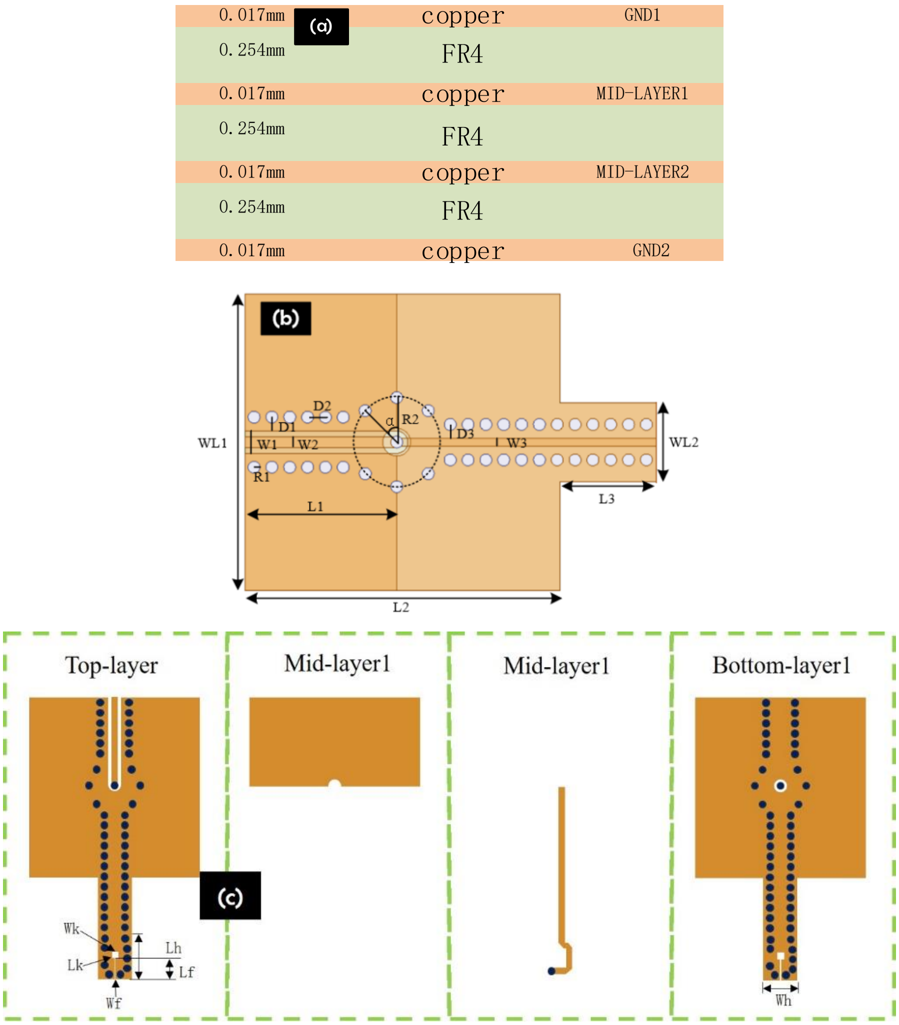

Fig. 2. Four-layer H-NF probe (a) laminated face view, (b) physical design parameters and (c) layered structure.

The physical sizes of the four-layer probe prototype are addressed in Tab. 1. The overall size of H-NF probe is 24.88 mm × 15 mm × 0.83 mm. The microwave circuit is implemented in four-layer PCB with the medium material is FR4 having relative permittivity 4.4 and loss tangent 0.02. For the implemented probe prototype, each layer thickness is 254 μm and the metal layer thickness is 17 μm. Moreover, the constituting four metal layers were designed to ensure the following roles:

- The top and bottom ones are the grounding layers for current return paths and EM shielding.
- The middle layer 1 is used to control the CPWG structure impedance.
- And the signal lines propagating through the middle layer 2 transmit the induced current to the receiving end.

The next subsection validates the H-NF probe characteristics with a standard test [25].

2.2 Validation of the Implemented Probe Prototype with H-NF Scanning from Standard Test Prototype

The H-NF probe performance indicators need to be measured through a standard microstrip line (ML) [29] with physical length $L = 80$ mm and characteristic impedance $R_0 = 50\ \Omega$ as DUT implemented on Cu-metallized Rogers 4350B substrate with thickness 1.524 mm and relative permittivity 3.66. Firstly, model the NF probe and a standard ML in simulation software, and place the probe directly above the center of the ML metal line. The bottom of the probe is perpendicular to the ML at 1-mm distance. The ML has two ports, one of which is the feeding port, set as Port 1, and the other is set as a $R_0 = 50\ \Omega$ matching load. The NF probe output port is set as Port 2. The probe and the DUT are simulated by HFSS® from Ansys® as shown in Fig. 3(a). The measurement of the H-NF probe is achieved through a vector network analyzer (VNA) and a standard ML.

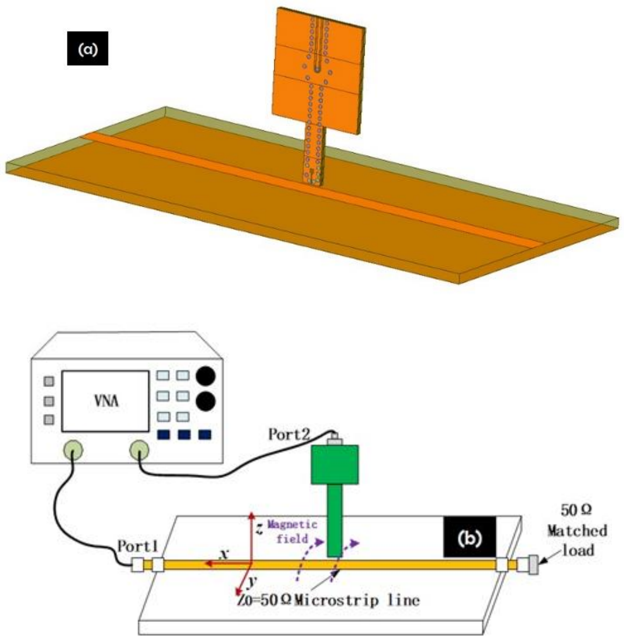

Fig. 3. (a) HFSS® 3-D design and (b) illustrative test diagram including VNA, probe and DUT.

The VNA Port 1 is connected to one end of the ML, Port 2 is connected to the H-NF probe, and the other end of the ML is connected to reference impedance R_0 as matching load, VNA obtains the return loss S_{22} of the probe output port and the transmission coefficient S_{21} between the probe and the ML. The probe connected to Port 2 is fixed vertically at height $z = 1$ mm above the metallization surface of the ML DUT. As shown by the test diagram of Fig. 3(b), the DUT and the probe were welded with SMA joint. For the test case illustrated by Fig. 3(b), the VNA referenced Keysight N9918A (Agilent) FieldFox with working frequency up to 26.5 GHz is connected to the DUT and the probe through standard short-open-load-thru (SOLT) calibration cables with characteristic impedance R_0. The photo of the DUT PCB implemented microstrip line for the standard NF emission is presented in Fig. 4. The H-NF probe has good frequency characteristics within 20 GHz BW.

The simulated (red lines) and measured (black lines) S-parameters are shown in Fig. 5. S_{21} (solid lines) and S_{22} (dashed lines) have good flatness, which can meet the measurement requirements of H-NF fields within 20 GHz. It is worth to note that the H-field captivated by the probe is extracted from S_{21}. In the high frequency range, there is a slight

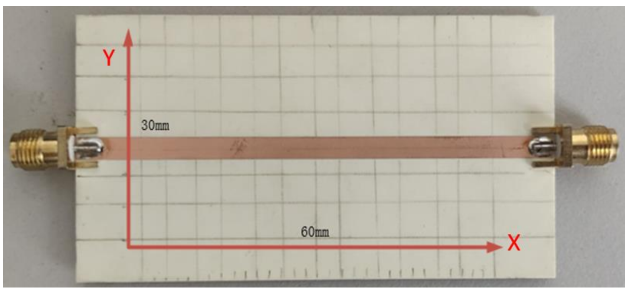

Fig. 4. Photograph of the DUT PCB for NF emission standard characterization test.

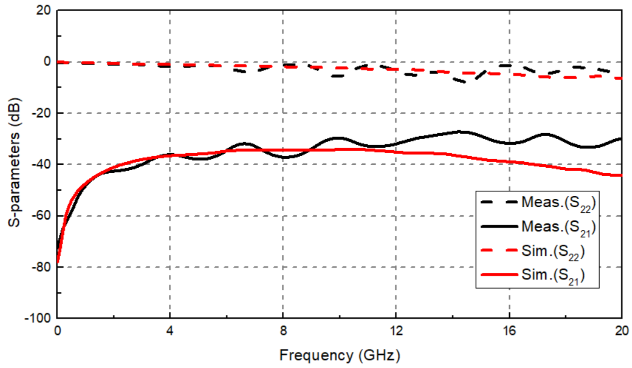

Fig. 5. Comparison of simulated and measured S-parameters of the H-NF probe.

error in the S-parameter of the probe, which is due to the fact that the electromagnetic field component in the measured environment is higher than the ideal environment in the simulation. At the same time, there are errors in the dielectric constant and loss tangent of the dielectric plate at high frequencies.

The spatial resolution reflects the ability of the H-NF probe to distinguish different field values. According to the IEC standard, place the probe 1 mm above the ML, move it along the normal direction of the metal line, record the values at different positions, and normalize them according to the maximum value of each frequency. The spatial resolution is the distance from the maximum value (usually located at the center of the ML) to the –6 dB attenuation position. As shown in Fig. 6, the spatial resolution of the proposed H-NF probe ranges from 1.27 mm to 181 mm within the frequency range of 5–20 GHz. Combined with the frequency response curve of the probe, the probe achieves good sensitivity and spatial resolution within the operating frequency range.

Usually, for H-NF probe, in order to measure more accurate magnetic field values, electric field suppression is also a noteworthy indicator. When the H-NF probe is placed as shown in Fig. 3, $\theta = 0°$, rotate the probe 90° along the z-axis, and then $\theta = 90°$. The electric field suppression is defined as the ratio of V_{21} ($\theta = 0°$) to V_{21} ($\theta = 90°$). The

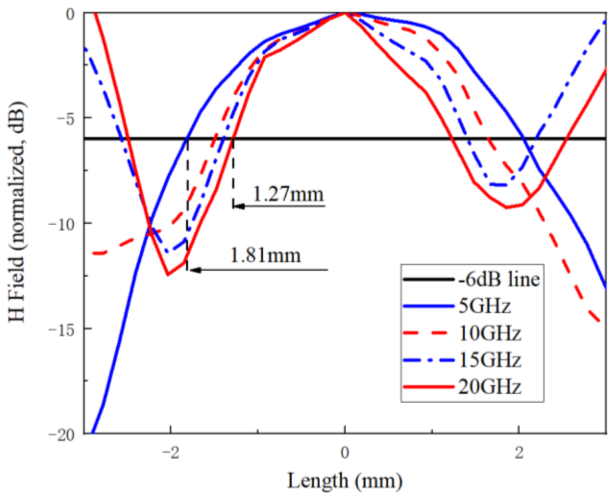

Fig. 6. The spatial resolution of the H-NF probe.

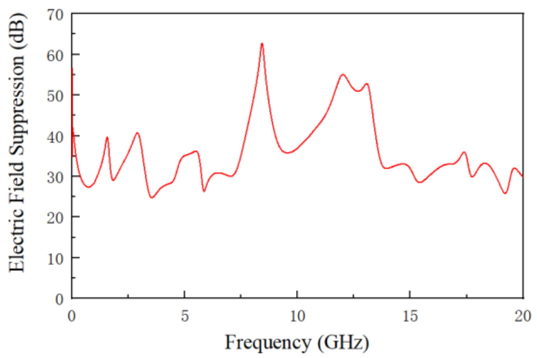

Fig. 7. The electric field suppression of the H-NF probe.

electric field suppression of H-NF probe is shown in Fig. 7. The electric field suppression of the probe is greater than 24.77 dB across all operating frequency ranges, demonstrating excellent electric field suppression characteristics.

The H-NF probe proposed in this article was compared with existing H-NF probes [30–33], as shown in Tab. 2. The flatness is defined as the fluctuation of S_{21} within a flat working range, and the smaller its value, the more stable the performance of the probe in the operating frequency band.

Compared with the existing ones, the H-NF probe under study is advantageous in terms of design simplicity, size smallness, flat frequency characteristics and electric field suppression. The measured results of the H-NF probe prototype for the IC and PCB EMC emission analysis are discussed in the next section.

3. Analysis of Measured IC Radiated Emission with the Developed NFS

As PoC, an IC test and analysis with the designed automated NFS are discussed in this section.

3.1 Design Description of the Automated NFS Installation

The self-developed NFS is shown Fig. 8 [29].

The personal computer (PC) is connected to the MCU by USB which is connected to the stepper motor driver through a serial port. The H-NF probe is fixed on the scanning platform and moves with the rotation of the stepped motor. The NFS practicality and aesthetics is considered in this design. A clear and user-friendly graphical interface has been designed on the front panel of LabVIEW®. In the NFS test system, vector network analyzer (VNA) and spectrum analyzer (SA) are the most commonly used measuring instruments. The Agilent® N9918A handheld radio frequency analyzer is selected as the test instrument, the frequency range is from 30 kHz to 26.5 GHz, and the VNA, SA and other modes are integrated. The test instrument control is realized based on Standard Commands for Programmable Instruments (SCPI). After receiving the data from the probe, the testing instrument communicates with the upper computer through the LAN port.

The following subsection will describe the operation conditioning of the tested IC integrated in a digital PCB.

3.2 STM32 IC DUT Operation Conditioning During the Test

The results of the MCU testing with the designed H-NF probe studied in the previous section and the NFS described in the previous subsection. During the experimentation, the DUT was energized and placed under the probe. The output end of the probe is connected to the spectrograph receiving port.

In the picture of Fig. 9, port A is the USB driver interface, and port B is the USB to serial port.

Reference	Maximum Frequency	Sensitivity and Flatness	Electric Field Suppression	Size
[30]	20 GHz	−27.15 dB ± 4.05 dB	≥ 22.52 dB	28 mm × 70 mm × 0.59 mm
[31]	10 GHz	−22.98 dB ± 2.90 dB	≥ 19.85 dB	15 mm × 48 mm × 1.035 mm
[32]	30 GHz	−38.89 dB ± 8.45 dB	≥ 12.25 dB	40 mm × 91.5 mm × 1.035 mm
[33]	16 GHz	−40.98 dB ± 4.70 dB	/	14.3 mm × 37.8 mm × 0.89 mm
This work	20 GHz	−30.93 dB ± 3.75 dB	≥ 24.77 dB	15 mm × 24.88 mm × 0.83 mm

Tab. 2. Comparison of NF probe performances.

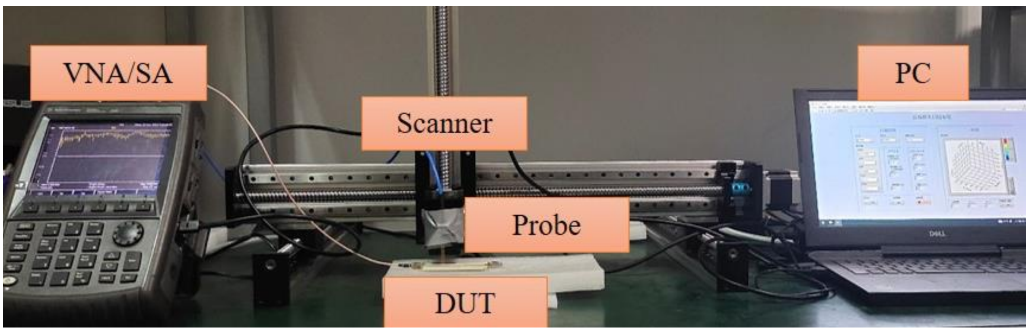

Fig. 8. Photograph of the NFS.

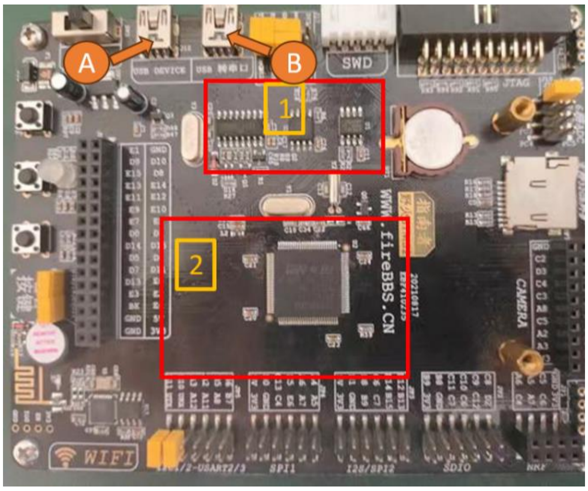

Fig. 9. Photo of the PCB DUT containing the IC under study.

According to the distribution of chips on the board, select two scanning areas:

- Area 1 mainly includes three types of chips. USB to serial port chips, serial FLASH chips, and electrically erasable programmable read only memory (EEPROM) chips. This area is mainly used for data communication and storage, as well as for clearing and rewriting MCU programs.
- Area 2 mainly includes the STM32 main chip and capacitor components distributed near the chip.

The measured H-NF emitted by the STM32 IC is discussed in the next subsection.

3.3 Discussion on the Measured H-NF Radiated by STM32 MCU IC DUT

The testing frequency as the chip's fundamental (main) and second harmonic frequency was considered during the test, respectively (f_1 = 72 MHz and f_2 = 144 MHz). The planar surface ranges of 30 mm × 20 mm and 50 mm × 30 mm were selected above Area 1 and Area 2 indicated in Fig. 9, respectively. During the NF test, the H-NF probe and MCU distance was z = 1 mm. Then, the scanning step was fixed to $\Delta x = \Delta y$ = 1 mm.

Firstly, the MCU is powered by a USB driver interface to obtain the H-NF distribution in some areas of the IC board, as shown in Fig. 10(a). From the above scanning results, when using the USB driver interface to power the MCU, there is no obvious H-NF radiation in the two scanning areas at the main frequency and second frequency points of the chip. The reason is that the MCU communication module is not enabled in this power supply method. In this case, the MCU does not support external data communication, and there is no high-speed signal transmission in the circuit. Then, power is supplied to the MCU through the USB to serial port, and the H-NF distribution in some areas of the MCU board is obtained as shown in Fig. 10(b) and Fig. 10(c). At this point, there is a clear magnetic field distribution above both scanning areas.

Comparing the power supply methods of USB driver interfaces, the MCU H-NF radiation distribution is very obvious under the power supply of USB to serial port. The main sources of radiation are high-speed clock signals and high-speed digital signals. In Area 1, due to the presence of chips such as TTL converted from serial port, it is an important module for the microcontroller to process communication data. During operation, there is a large amount of high-speed signal transmission, which will generate obvious electromagnetic radiation.

In Area 2, there is also obvious radiation at some pins of the chip and nearby capacitors. The upper part of the chip is close to the crystal oscillator, where there is strong radiation. The capacitors near the chip are decoupling capacitors, which are placed near the chip power supply pins. By diverting the current flowing to the power supply, the chip avoids voltage fluctuations. Therefore, EM radiation also exists at the decoupling capacitors. In addition, compared with the magnetic field distribution at the chip main frequency of f_1, the magnetic field radiation intensity in the selected scanning area is stronger and wider at the chip second harmonic frequency of f_2. On the one hand, this is because at low frequencies, the length of the circuit is shorter than the wavelength of the electromagnetic wave, making it difficult to form a radiation antenna. When the frequency increases and the wavelength is shortened, some circuits will form an antenna structure generating EM radiation.

On the other hand, there are nonlinear components on the circuit board, and the signal may generate large harmonics when passing through the nonlinear components. In addition, there are parasitic inductors and capacitors in the circuit during operation. When the resonant frequency of these parasitic components is the same as the chip second harmonic frequency, significant radiation will also be generated.

4. Conclusion

A miniaturized broadband H-NF probe with a four-layer PCB structure was proposed, and the probe was measured and verified based on the IEC-61967 standard. The proposed probe has a working frequency of up to 20 GHz and has the advantages of high sensitivity, high flatness, and high electric field suppression. Based on the self-developed NFS, the proposed probe is used to perform near-field scanning testing and analysis on an active IC circuit. A very good result of H-NF mapping at different test frequencies f_1 and f_2 showing the influence of parasitic harmonic EMC radiation was observed.

In the future, the NFS test results open different perspectives of EMC emission measurement for complex IC and PCBs with more comprehensive and accurate practical analysis. Moreover, the developed NFS can be exploited to characterize the EMC characteristics of mobile communication devices as smartphones, smart car and aeronautics electronic devices at higher frequencies.

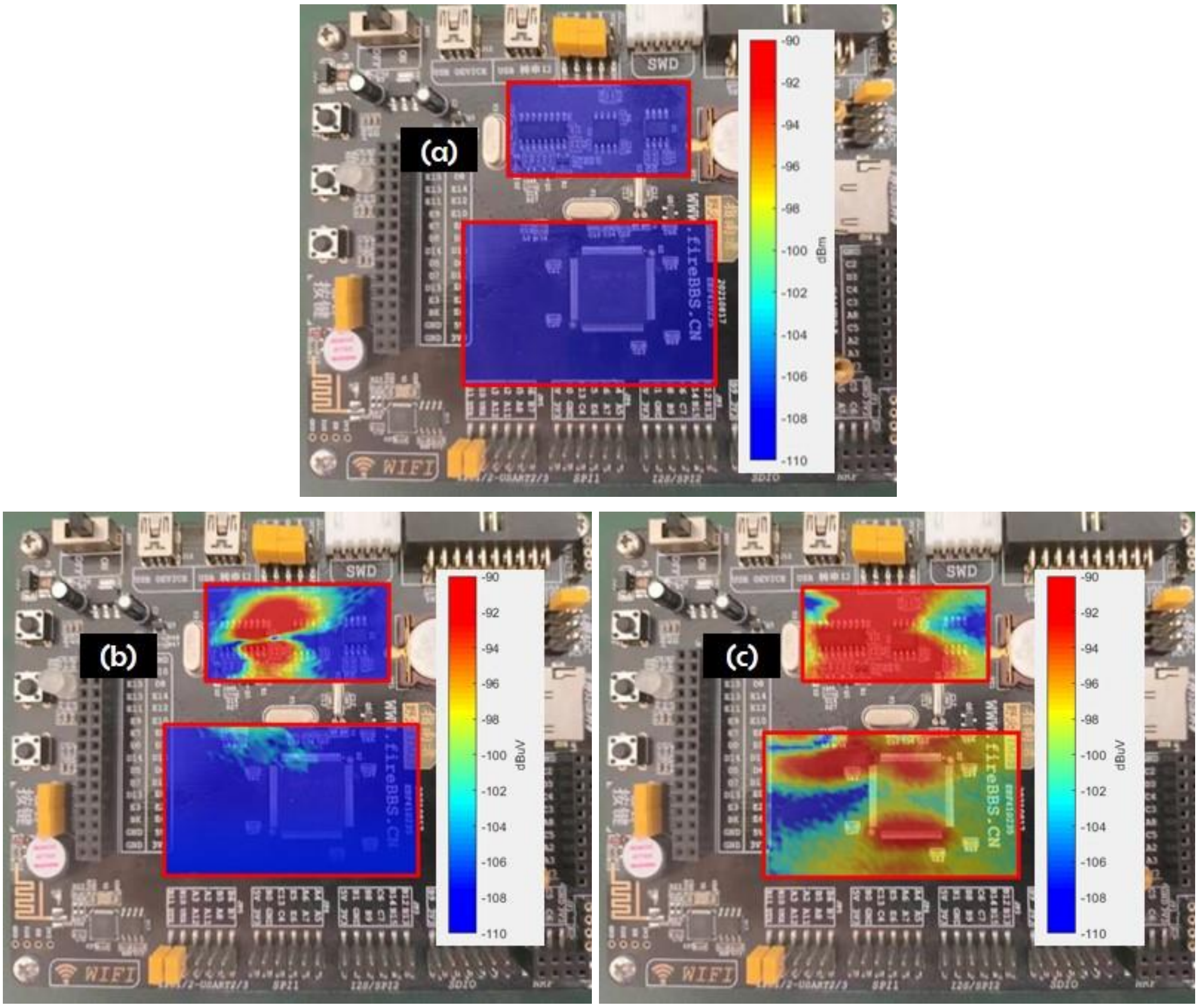

Fig. 10. H-NF mappings from DUT shown in Fig. 9 at (a) f_1 and f_2 from DUT powered by USB driver interface, and (b) f_1 and (c) f_2 from DUT powered by USB to serial port.

Acknowledgments

This research work is supported in part by Natural National Science Foundation of China (NSFC) under Grant No. 62350610268 and in part by Beijing Natural Science Foundation under Grant L233002.

References

[1] WU, T.-L., BUESINK, F., CANAVERO, F. Overview of signal integrity and EMC design technologies on PCB: Fundamentals and latest progress. *IEEE Transactions on Electromagnetic Compatibility*, 2013, vol. 55, no. 4, p. 624–638. DOI: 10.1109/TEMC.2013.2257796

[2] HUANG, Q., ZHANG, L., RAJAGOPALAN, J., et al. A novel RFI mitigation method using source rotation. *IEEE Transactions on Electromagnetic Compatibility*, 2021, vol. 63, no. 1, p. 11–18. DOI: 10.1109/TEMC.2020.2995828

[3] WEI, X., DING, L., WEN, J., et al. Review of near-field EMI measurement. In *International Conference on Microwave and Millimeter Wave Technology (ICMMT)*. Shanghai (China), 2020, p. 1–3. DOI: 10.1109/ICMMT49418.2020.9387013

[4] XU, Y., FU, H., XUANYUAN, Y., et al. Wireless coexistence testing and EMC risk evaluation for wireless medical applications. In *Advanced Science and Industry Research Center. Proceedings of 2018 International Conference on Energy, Power, Electrical and Environmental Engineering (EPEEE 2018)*. Wuhan (China), 2018, p. 241–245.

[5] MIRANDA, J., CABRAL, J., RAVELO, B., et al. Radiated EMC immunity investigation of Common Recognition Identification Platform for medical applications. *European Physical Journal, Applied Physics*, 2015, vol. 69, no. 1, p. 1–8. DOI: 10.1051/epjap/2014140230

[6] SONG, E., PARK, H., PARK, H. H. An evaluation method for radiated emissions of components and modules in mobile devices. *IEEE Transactions on Electromagnetic Compatibility*, 2014, vol. 56, no. 5, p. 1020–1026. DOI: 10.1109/TEMC.2014.2307915

[7] LEMAN, S., DEMOULIN, B., MAURICE, O., et al. New approaches in electromagnetic compatibility: Use of the circuit approach to solve large EMC problems. *C. R. Physique*, 2019, vol. 10, no. 1, p. 70–82. DOI: 10.1016/j.crhy.2009.01.006

[8] AUNCHALEEVARAPAN, K., PAITHOONWATANAKIJ, K., KHAN-NGERN, W., et al. Novel method for predicting PCB

configurations for near-field and far-field radiated EMI using a neural network. *IEICE Transactions on Communications*, 2003, vol. E86-B, no. 4, p. 1364–1376. ISSN: 0916-8516

[9] MUNIC, N., NIKOLIC STEVANOVIC, M., DJORDJEVIC, A., et al. Evaluation of radiating-source parameters by measurements in Faraday cages and sparse processing. *Measurement*, 2017, vol. 104, p. 105–116. DOI: 10.1016/j.measurement.2017.03.008

[10] BOYER, A., NOLHIER, N., CAIGNET, F., et al. On the correlation between near-field scan immunity and radiated immunity at printed circuit board level - Part I. *IEEE Transactions on Electromagnetic Compatibility*, 2022, vol. 64, no. 4, p. 1230–1242. DOI: 10.1109/TEMC.2022.3169183

[11] BOYER, A., NOLHIER, N., CAIGNET, F., et al. On the correlation between near-field scan immunity and radiated immunity at printed circuit board level - Part II. *IEEE Transactions on Electromagnetic Compatibility*, 2022, vol. 64, no. 5, p. 1493–1505. DOI: 10.1109/TEMC.2022.3172601

[12] HUANG, Q., CHEN, R., FANG, W., et al. Radiation emission source localization by magnetic near-field mapping along the surface of a large-scale IC with BGA package. *IEEE Transactions on Electromagnetic Compatibility*, 2022, vol. 64, no. 2, p. 495–505. DOI: 10.1109/TEMC.2021.3123536

[13] DING, L., XU, Z. EMI source positioning by phase inversion and near-field scanning. In *Asia-Pacific International Symposium on Electromagnetic Compatibility (APEMC)*. Beijing (China), 2022, p. 69–71. DOI: 10.1109/APEMC53576.2022.9888587

[14] WHITESIDE, H., KING, R. The loop antenna as a probe. *IEEE Transactions on Antennas and Propagation*, 1964, vol. 12, no. 3, p. 291–297. DOI: 10.1109/TAP.1964.1138213

[15] CHO, G. Y., JIN, J., PARK, H., et al. Assessment of integrated circuits emissions with an equivalent dipole-moment method. *IEEE Transactions on Electromagnetic Compatibility*, 2017, vol. 59, no. 2, p. 633–638. DOI: 10.1109/TEMC.2016.2633332

[16] RAVELO, B. Non-unicity of the electric near-field planar emission model with dipole array. *IET Microwaves, Antennas & Propagation*, 2017, vol. 11, no. 5, p. 584–592. DOI: 10.1049/iet-map.2016.0910

[17] LIU, Y., RAVELO, B., JASTRZEBSKI, A. K. Time-domain magnetic dipole model of PCB near-field emission. *IEEE Transactions on Electromagnetic Compatibility*, 2016, vol. 58, no. 5, p. 1561–1569. DOI: 10.1109/TEMC.2016.2578953

[18] RAVELO, B., LIU, Y., JASTRZEBSKI, A. K. PCB near-field transient emission time-domain model. *IEEE Transactions on Electromagnetic Compatibility*, 2015, vol. 57, no. 6, p. 1320–1328. DOI: 10.1109/TEMC.2015.2438053

[19] KIM, J., KIM, W., YOOK, J. Resonance-suppressed magnetic field probe for EM field-mapping system. *IEEE Transactions on Microwave Theory and Techniques*, 2005, vol. 53, no. 9, p. 2693–2699. DOI: 10.1109/TMTT.2005.854203

[20] YANG, S., HUANG, Q., LI, G., et al. Differential E-field coupling to shielded H-field probe in near-field measurements and a suppression approach. *IEEE Transactions on Instrumentation and Measurement*, 2018, vol. 67, no. 12, p. 2872–2880. DOI: 10.1109/TIM.2018.2831398

[21] LIU, Y., RAVELO, B. Fully time-domain scanning of EM near-field radiated by RF circuits. *Progress In Electromagnetics Research B*, 2014, vol. 57, p. 21–46. DOI: 10.2528/PIERB13072903

[22] YAN, Z., WANG, J., ZHANG, W., et al. A simple miniature ultrawideband magnetic field probe design for magnetic near-field measurements. *IEEE Transactions on Antennas and Propagation*, 2016, vol. 64, no. 12, p. 5459–5465. DOI: 10.1109/TAP.2016.2606556

[23] LIU, W., YAN, Z., MIN, Z., et al. Design of miniature active magnetic probe for near-field weak signal measurement in ICs. *IEEE Microwave and Wireless Components Letters*, 2020, vol. 30, no. 3, p. 312–315. DOI: 10.1109/LMWC.2020.2967384

[24] YANG, R., WEI, X., SHU, Y., et al. A miniature multi-component probe for near-field scanning. *IEEE Transactions on Antennas and Propagation*, 2019, vol. 67, no. 11, p. 6821–6828. DOI: 10.1109/TAP.2019.2927814

[25] INTERNATIONAL ELECTROTECHNICAL COMISSION. *Integrated Circuits–Measurement of Electromagnetic Emissions, IEC-61967*, 2011.

[26] SUDO, T. Predicting common mode radiation of power bus structure excited by IC's switching current. In *Asia-Pacific Symposium on Electromagnetic Compatibility and 19th International Zurich Symposium on Electromagnetic Compatibility*. Singapore, 2008, p. 160–163. DOI: 10.1109/APEMC.2008.4559836

[27] CHEN, L., WU, J., ZHANG, H., et al. An optimized test method based on IC-Stripline TEM Cell. In *Asia-Pacific International Symposium on Electromagnetic Compatibility (APEMC)*. Nusa Dua–Bali (Indonesia), 2021, p. 1–4. DOI: 10.1109/APEMC49932.2021.9596990

[28] FANG, W., EN, Y., HUANG, Y., et al. Extracting the electromagnetic radiated emission source of an integrated circuit by rotating the test board in a TEM cell measurement. *IEEE Transactions on Electromagnetic Compatibility*, 2019, vol. 61, no. 3, p. 933–841. DOI: 10.1109/TEMC.2018.2836698

[29] JIA, H., WAN, F., CHENG, X., et al. Electric near-field scanning for electronic PCB electromagnetic radiation measurement. *Measurement*, 2024, vol. 228, p. 1–9. DOI: 10.1016/j.measurement.2024.114355

[30] SHAO, W., FANG, W., CHEN, R., et al. Magnetic near-field measurement with a differential probe to suppress common mode noise. *IEEE Sensors Journal*, 2019, vol. 19, no. 21, p. 9697–9703. DOI: 10.1109/JSEN.2019.2928853

[31] YAN, Z., LIU, W., WANG, J., et al. Noncontact wideband current probes with high sensitivity and spatial resolution for noise location on PCB. *IEEE Transactions on Instrumentation and Measurement*, 2018, vol. 67, no. 12, p. 2881–2891. DOI: 10.1109/TIM.2018.2830859

[32] YANG, R., WEI, X., SHU, Y., et al. A high-frequency and high spatial resolution probe design for EMI prediction. *IEEE Transactions on Instrumentation and Measurement*, 2019, vol. 68, no. 8, p. 3012–3019. DOI: 10.1109/TIM.2018.2869181

[33] WANG, L., LIU, X., LU, G., et al. A new differential magnetic-field probe with parasitic elements for near-field scanning. *IEEE Photonics Journal*, 2024, vol. 16, no. 3, p. 1–5. DOI: 10.1109/JPHOT.2024.3391012

About the Authors …

Hongchuan JIA was born in China. He received the B.Eng. degree in Communication Engineering in 2021 from the Nanjing University of Information Science and Technology, Nanjing, China, where he is currently working toward the Ph.D. degree. His research interests include the EMC engineering, near-field (NF) scanner (NFS) development and multi-layer NF probe design for PCB radiating emission analysis.

Fayu WAN (corresponding author) was born in China. He received the Ph.D. degree in Electronic Engineering from the University of Rouen, Rouen, France, in 2011. From 2011 to 2013, he was a Postdoctoral Fellow with the Electromagnetic Compatibility Laboratory, Missouri University of Science and Technology, Rolla, MO, USA. He is currently a Full Professor with the Nanjing University of Information Science and Technology, Nanjing, China. His research interests include negative group delay circuits, electrostatic discharge, electromagnetic compatibility, and advanced RF measurement.

Vladimir MORDACHEV was born in in Vitebsk, Belarus. He received the M.S. degree (with honors) and the Ph.D. degree in Radio Engineering from the Minsk Radio Engineering Institute, Minsk, Belarus, in 1974 and 1984, respectively. He received an academic rank of Senior Scientist in 1985. His current research interests include spectrum management, wireless communications and networks, electromagnetic compatibility and interference, wireless network planning, computer-aided analysis and design, cellular networks system ecology, RF systems modeling, and simulation. He is extensively involved in consulting to wireless network operators, industry and the local government. He is the Head of the Electromagnetic Compatibility Laboratory, Belarusian State University of Informatics and Radioelectronics, Minsk, Belarus.

Eugene SINKEVICH received the M.S. degree in Radio System Engineering (summa cum laude) from the Belarusian State University of Informatics and Radioelectronics (BSUIR), Minsk, Belarus, in 2000. From 2000 to 2003, he was with the Department of Radio Engineering Theory, BSUIR. From 2004 to 2005, he was with the Department of Radio Devices, BSUIR. Since 2005, he is with the EMC R&D Laboratory, BSUIR, where he is currently the Senior Researcher, Team Leader, and Principal Designer of international R&D projects. His current research interests include electromagnetic compatibility, RF and microwave measurements, and wireless systems and devices. He is the author of about 20 technical papers on international journals and conference proceedings.

Jérôme ROSSIGNOL received the M.S. degree in Physics and the Ph.D. degree in Plasma Physics from Université Blaise Pascal (Clermont Ferrand) in 1998 and 2001, respectively. He has been working with the Humbolt University, Berlin, Germany, as a Postdoctoral Fellow, with ITER international project. Since 2002, he has been an Associate Professor in electronic and microwave systems with the Université de Bourgogne-Franche-Comté, affiliated with the GERM Microwave Team, Interface Department of ICB UMR 6303, Dijon, France. His current research interests include microwaves matter interactions, microwaves transduction and imagery, and nanomaterials for sensing. He has coauthored more than 33 peer-reviewed articles and 25 communications in international conferences, and he is co-inventor of one patent.

Xiaohe CHEN received the Ph.D. degree from Missouri University of Science and Technology in 2007; since 2007, he has been working as a director system architect in the Design Analysis and Product Blueprinting Department at Apple HQ; in 2015, he has been working as the director of the Electromagnetic Compatibility Research Center of Suzhou Institute of Biomedical Engineering and Technology, Chinese Academy of Sciences, and the director of the Research Laboratory of Medical Electronics; and he will be a professor and a doctoral director at the School of Informatics, China University of Petroleum, China, in 2022. His research interests are biomedical informatics, artificial intelligence, signal processing, signal integrity research, electromagnetic compatibility.

Blaise RAVELO is currently a University Full Professor with the Nanjing University of Information Science and Technology, Nanjing, China. He supervised ten Ph.D. students. He has coauthored more than 430 scientific research papers in new technologies published in international conference and journals. His research interests include multiphysics modeling, Kron's method, RF/electronics engineering, EMC/SI/PI of PCBs, and pioneer of the negative group delay theory, engineering and application for data prediction. With international partners, he is actively involved and contributes on several international research projects. He is an Associate Editor and the Circuit and System Subject Editor of the Editorial Board of IET Electronics Letters, and Associate Editor of Advanced Electromagnetics journal. He is a Member of Scientific Technical Committee of International Conference on Antennas and Electromagnetic Systems. He is ranked in Top 2% world’s scientists based on years (during 2020–2024) by Stanford University, U.S. He has Google scholar H-index(2025) = 32 and i10-index(2025) = 117. He is a member of research groups: URSI, GDR Ondes, Radio Society.